THE JOURNAL OF BIOLOGICAL CHEMISTRY
Vol. 280, No. 14, Issue of April 8, pp. 13962–13972, 2005
Printed in U.S.A.

A New Type of Peroxisomal Acyl-Coenzyme A Synthetase from *Arabidopsis thaliana* Has the Catalytic Capacity to Activate Biosynthetic Precursors of Jasmonic Acid*

Received for publication, December 2, 2004, and in revised form, January 19, 2005
Published, JBC Papers in Press, January 26, 2005, DOI 10.1074/jbc.M413578200

Katja Schneider‡, Lucie Kienow‡, Elmon Schmelzer‡, Thomas Colby‡, Michael Bartsch‡, Otto Miersch§, Claus Wasternack§, Erich Kombrink‡¶, and Hans-Peter Stuible‡

From the ‡Max Planck Institute for Plant Breeding Research, Department of Plant-Microbe Interactions, Carl-von-Linné-Weg 10, 50829 Köln and the §Leibniz Institute of Plant Biochemistry, Department of Natural Product Biotechnology, Weinberg 3, 06120 Halle, Germany

Arabidopsis thaliana **contains a large number of genes that encode carboxylic acid-activating enzymes, including nine long-chain fatty acyl-CoA synthetases, four 4-coumarate:CoA ligases (4CL), and 25 4CL-like proteins of unknown biochemical function. Because of their high structural and sequence similarity with *bona fide* 4CLs and their highly hydrophobic putative substrate-binding pockets, the 4CL-like proteins At4g05160 and At5g63380 were selected for detailed analysis. Following heterologous expression, the purified proteins were subjected to a large scale screen to identify their preferred *in vitro* substrates. This study uncovered a significant activity of At4g05160 with medium-chain fatty acids, medium-chain fatty acids carrying a phenyl substitution, long-chain fatty acids, as well as the jasmonic acid precursors 12-oxo-phytodienoic acid and 3-oxo-2-(2′-pentenyl)-cyclopentane-1-hexanoic acid. The closest homolog of At4g05160, namely At5g63380, showed high activity with long-chain fatty acids and 12-oxo-phytodienoic acid, the latter representing the most efficiently converted substrate. By using fluorescent-tagged variants, we demonstrated that both 4CL-like proteins are targeted to leaf peroxisomes. Collectively, these data demonstrate that At4g05160 and At5g63380 have the capacity to contribute to jasmonic acid biosynthesis by initiating the β-oxidative chain shortening of its precursors.**

The activation of carboxylic acids is required in numerous metabolic pathways of all organisms and contributes to the biosynthesis or degradation of diverse compounds such as fatty acids, amino acids, and a variety of secondary metabolites. Despite the structural diversity of their substrates, many enzymes acting on carboxylic acids utilize the same ATP-dependent two-step mechanism. The first step is characterized by the formation of an acyl-AMP intermediate, the so-called adenylate, with concomitant release of pyrophosphate (Reaction 1).

$$\text{Acid} + \text{ATP} \rightarrow \text{acyl-AMP} + \text{PP}_i$$

REACTION 1

In the second step, the acyl group is transferred to an ultimate acceptor, which in most cases is CoA, and AMP is released (Reaction 2).

$$\text{Acyl-AMP} + \text{CoA} \rightarrow \text{acyl-CoA} + \text{AMP}$$

REACTION 2

A large number of enzymes catalyzing the above reaction sequence are characterized by the presence of a highly conserved putative AMP-binding domain (PROSITE PS00455), and in fact, this sequence motif has been used to group diverse proteins such as fatty acyl-CoA synthetases, acetyl-CoA synthetases, 4-coumarate:CoA ligases, chlorobenzoate:CoA ligase, nonribosomal polypeptide synthetases, and firefly luciferases in one superfamily of adenylate-forming enzymes (1, 2).

In *Arabidopsis thaliana* 44 genes have been identified that encode proteins containing the consensus AMP-binding domain signature, whereas 19 additional genes contain a more distantly related sequence motif (3, 4). For some members of the latter group, the ATP-dependent *in vitro* adenylation of the plant hormones jasmonic acid (JA),[1] salicylic acid, or indole-3-acetic acid (IAA) has been demonstrated, and hence a function in hormone signaling was inferred (3). Recently, it was shown that one enzyme of this group, called JAR1, functions as a JA-amino acid synthetase conjugating activated JA with isoleucine, and genetic evidence supports the notion that JA-Ile is indeed an essential component of jasmonate signaling in *Arabidopsis* (5). In contrast to JA, amino acid conjugates of IAA have been known for a long time, but the enzymes responsible for their biosynthesis have not yet been reported.

Among the 44 *Arabidopsis* proteins containing the consensus AMP-binding domain, several fatty acyl-CoA synthetases differing in chain length specificity and cellular localization, four 4-coumarate:CoA ligases (4CLs), and one acetyl-CoA synthetase have been identified, but the function of the remaining enzymes is still unknown (4, 6–13). Two of the nine long-chain fatty acyl-CoA synthetases (LACS) present in *Arabidopsis*, LACS6 and LACS7, represent peroxisomal enzymes that are essential for storage lipid mobilization during germination (12, 13). Hence a *lacs6 lacs7* double mutant requires exogenous

* This work was supported by Deutsche Forschungsgemeinschaft Grant KO1192/6-1/2. The costs of publication of this article were defrayed in part by the payment of page charges. This article must therefore be hereby marked "*advertisement*" in accordance with 18 U.S.C. Section 1734 solely to indicate this fact.

¶ To whom correspondence should be addressed. Tel.: 49-221-5062-320; Fax: 49-221-5062-353; E-mail: kombrink@mpiz-koeln.mpg.de.

[1] The abbreviations used are: JA, jasmonic acid; IAA, indole-3-acetic acid; MeJA, methyl jasmonate; 4CL, 4-coumarate:CoA ligase; LACS, long-chain fatty acyl-CoA synthetase; OPDA, 12-oxo-phytodienoic acid; OPC-8:0, 3-oxo-2-(2′-pentenyl)-cyclopentane-1-octanoic acid; OPC-6:0, 3-oxo-2-(2′-pentenyl)-cyclopentane-1-hexanoic acid; OPR-3, OPDA reductase-3; SBP, substrate-binding pocket; PTS1, peroxisomal targeting signal type 1; IBA, indole-butyric acid; RFP, red fluorescent protein; YFP, yellow fluorescent protein; MS, mass spectrometry; WT, wild type; RT, reverse transcriptase.

sucrose for germination and seedling development (13), a phenotype also described for the *Arabidopsis pxa1* mutant and other mutants defective in β-oxidation (14–16). The PXA1 protein is an ATP-binding cassette transporter located in the peroxisomal membrane and considered to import long-chain fatty acid CoA esters for β-oxidation from the cytosol (14). The observation that the *pxa1* mutant and the *lacs6 lacs7* double mutant are compromised in the mobilization of storage lipids indicates that both activated and free fatty acids are imported into peroxisomes and that peroxisomal LACS activity is essential for plant β-oxidation to support early seedling growth (13).

Plant peroxisomes are involved in a variety of oxidative processes such as the β-oxidation of fatty acids to produce acetyl-CoA, the metabolism of glycolate formed during photorespiration, and the catabolism of aliphatic amino acids (17–19). In addition, peroxisomal enzymes contribute to the formation and turnover of signaling molecules such as nitric oxide and H_2O_2 (20) and to the biosynthesis of the plant hormones IAA and JA (21–24). Analogous to the mammalian eicosanoid pathway, the biosynthesis of JA in *Arabidopsis* occurs via the octadecanoic pathway starting from linolenic acid (18:3) or, alternatively, via the hexadecanoid pathway starting from hexadecatrienoic acid (16:3) (25, 26). In leaves, these polyunsaturated fatty acids may be released from the membrane lipids of the chloroplast by phospholipases functionally related to DAD1 (27), and in subsequent steps, they are converted to the cyclopentenones 12-oxo-phytodienoic acid (OPDA) or dinor-OPDA, respectively, by the enzymes lipoxygenase, allene oxide synthase, and allene-oxide cyclase (25, 28, 29). OPDA may then be re-esterified to plastid-specific galactolipids (30) or may be released from the chloroplast and function as a signal molecule mediating mechanotransductory processes or plant defense responses (30, 31). For conversion to JA, OPDA or an OPDA derivative has to be translocated into peroxisomes where it is reduced to 3-oxo-2-(2′-pentenyl)-cyclopentane-1-octanoic acid (OPC-8:0) by OPDA reductase-3 (OPR-3), the action of which is followed by three rounds of β-oxidation (22, 25, 32, 33). This sequence of β-oxidative steps is indicated by the fact that only even-numbered carboxylic acid side chains of OPC derivatives led to JA biosynthesis (34). In contrast to all other steps of JA biosynthesis, enzymes participating in these β-oxidative reactions of JA precursors have not yet been identified or characterized.

Four isoforms of 4-coumarate:CoA ligase (4CL) have been identified in *Arabidopsis*, which presumably constitute the complete enzyme family (6, 9). Typically, 4CLs activate 4-coumaric, caffeic, and ferulic acid to the corresponding CoA esters. These activated cinnamic acid derivatives serve as precursors for the biosynthesis of numerous plant secondary compounds such as flavonoids, isoflavonoids, coumarins, lignin, suberin, anthocyanins, and wall-bound phenolics, which have essential functions in plant development and environmental interactions (35, 36). We have shown previously that the four *Arabidopsis* 4CL isoforms exhibit distinct substrate utilization profiles that may be related to specific metabolic functions (6). By detailed biochemical characterization of At4CL2, a naturally occurring loss-of-function mutant that is incapable of converting ferulic acid, and homology modeling of its substrate-binding pocket (SBP), we uncovered the substrate specificity-determining amino acid code of 4CLs (37). This specificity code allowed the rational design of At4CL2 variants with new catalytic properties, including the capacity to activate ferulic, sinapic, and cinnamic acid, substrates not normally converted by the At4CL2 wild-type enzyme (37).

In extension of this work, we are now exploring the structure-function relationship of 4CL-like proteins that are amply encoded by the *Arabidopsis* genome (4, 37). It has been suggested that 4CL-like proteins may activate cinnamic, benzoic, or fatty acid derivatives, including precursors of plant hormones, but no such enzymatic function has yet been demonstrated for any of these proteins (4, 37, 38). Ideally, direct transfer of structural information from the 4CL system to 4CL-like proteins would lead to a defined arrangement of amino acid residues forming the putative SBP, thereby delimiting the space and chemical environment for a potential substrate. However, structure prediction is still a challenging task, and in case of the 4CL-like proteins further hampered by the occurrence of insertions and deletions in the region comprising the putative SBP-forming amino acid residues. Therefore, we developed a luciferase-based assay that is generally applicable to adenylate-forming enzymes and allows the semi-quantitative analysis of their *in vitro* substrate utilization at a large scale. By applying this screen to two 4CL-like proteins from *Arabidopsis*, At4g05160 and At5g63380, we uncovered that both enzymes have the capacity to activate different fatty acid derivatives, including the JA precursors OPDA and 3-oxo-2-(2′-pentenyl)-cyclopentane-1-hexanoic acid (OPC-6:0). Together with their demonstrated localization in peroxisomes, these catalytic activities suggest that both enzymes have a function in JA biosynthesis.

EXPERIMENTAL PROCEDURES

Isolation and Cloning of At4g05160 and At5g63380 cDNAs—The cDNAs of At4g05160 and At5g63380 were amplified by RT-PCR from *A. thaliana* (Col-0) total RNA. Synthesis of the cDNAs and subsequent PCR amplification of the full-length reading frames was performed with the Titan® one tube RT-PCR kit (Roche Diagnostics) according to the manufacturer's instructions with the primer pair At4g05160-FI and -RI (ATGGAGAAATCCGGCTACGGCAGAGACG and TCACATCTTGGATCTTACTTGCTGAACAAG) and the primer pair At5g63380-FI and -RI (ATGCTGACGAAAACCAACGACAGC and TCAAAGTTTTGATGCATTGCCATCCAC), respectively. The resulting cDNAs were used as templates for a second round of PCR amplification using the primer pair At4g05160-FII and -RII (ATCTTAACAAGCATGCCGAAATCCGGCTACGGCAGAGACGGAATTTAC and TATTAATTAGTCGACTCACATCTTGGATCTTACTTGCTGAACAAGTTC) and the primer pair At5g63380-FII and -RII (TTAAATGGATCCATGCTGACGAAAACCAACGACAGCCG and AATTAAGTCGACTCAAAGTTTTGATGCATTGCCATCCACAGC), respectively. In the case of At4g05160, this second PCR amplification was used to introduce the SphI and SalI sites required for cloning into the expression vector pQE32 (Qiagen, Hilden, Germany). In case of At5g63380, BamHI and SalI sites were introduced in the second round of PCR amplification, and the resulting product was cloned into the expression plasmid pQE30 (Qiagen, Hilden, Germany). The DNA sequences of all isolated clones were determined by the ADIS service unit (Max Planck Institute for Plant Breeding Research, Köln, Germany) on ABI PRISM377 DNA sequencers (PE Applied Biosystems, Foster City) by using BigDye Terminator chemistry and were found to be identical with the sequences available from the MIPS data base (Munich Information Center for Protein Sequences, Neuherberg, Germany).

Heterologous Expression and Purification of At4g05160 and At5g63380—Expression and purification of At4g05160 and At5g63380 were essentially carried out as described previously for At4CL2 (2), with the exception that the expression plasmids were introduced into the *Escherichia coli* strain DH5α carrying the repressor plasmid pREP4 (Qiagen, Hilden, Germany) and that the growth temperature was reduced to 25 °C. The purity of the enzymes was inspected by SDS gel electrophoresis. Protein concentrations were determined according to Bradford (39) with bovine serum albumin as standard.

4CL-catalyzed Synthesis of CoA Esters—4CL activity was determined by the spectrophotometric assay described previously (6) with standard concentrations of the cinnamic acid derivative (0.2 mM), ATP (5.5 mM), and CoA (0.3 mM). The specific increase of absorbance during CoA ester formation was monitored at wavelengths of 311, 333, 363, 345, and 352 nm for cinnamoyl-CoA, 4-coumaroyl-CoA, caffeoyl-CoA, feruloyl-CoA, and sinapoyl-CoA, respectively, and the appropriate molar extinction coefficients were used for calculating activity (40, 41).

Luciferase-based Assay of Adenylate-forming Enzymes—To screen a large number of carboxylic acids for activation by 4CL and 4CL-like proteins, the decrease in ATP concentration was determined by a lucif-

erase-coupled assay. The standard reaction mixture contained 2 μg of purified protein, 200 μM carboxylic acid substrate, 50 μM ATP, 250 μM $MgCl_2$, 100 μM CoA, 1 mM dithioerythritol, and 0.1 M Tris-HCl (pH 7.5) in a total volume of 200 μl. Highly lipophilic substrates, such as long-chain fatty acids, were dissolved in buffer containing 2% Triton X-100, leading to a final concentration of 0.1% Triton X-100 in the assay. Jasmonic acid precursors were first dissolved in EtOH and subsequently diluted with detergent-containing buffer, leading to final concentrations of 0.1% EtOH and 0.1% Triton X-100 in the assay. The reaction mixtures were incubated at room temperature, and for ATP determination, 2-μl samples were withdrawn at various time points and added to a reaction mixture containing 1 μg of firefly luciferase (Roche Diagnostics), 4.6 μg of luciferin (Roche Diagnostics), and 0.1 M Tris-HCl (pH 7.8) in total volume of 200 μl. Photon emission was measured for 10 s with a Lumat LB 9501 luminometer (Berthold Technologies, Bad Wildbad, Germany) and expressed as relative luciferase activity, which is directly proportional to ATP concentration. To minimize the variability of the assay, all ATP determinations were normalized to a reaction containing At4CL2 and sinapic acid, in which no ATP depletion occurred and correspondingly was set to 100%. Time course experiments using At4CL2 showed that good substrates resulted in significant ATP depletion within 1–4 h (not shown). Therefore, an incubation period of 2 h was chosen for the large scale screen.

Coupled Enzyme Assay of Acyl-CoA Synthetases—For detailed kinetic analyses, the activation of selected substrates to the corresponding CoA esters by At4g05160 and At5g63380 was followed by measuring AMP formation in a coupled spectrophotometric assay with myokinase, pyruvate kinase, and lactate dehydrogenase adapted from Ziegler *et al.* (42). The reaction mixture (1 ml) contained 0.1 M Tris-HCl (pH 7.5), 2 mM dithioerythritol, 5 mM ATP, 10 mM $MgCl_2$, 0.5 M CoA, 0.1 mM NADH, 1 mM phosphoenolpyruvate, 12 nanokatal of myokinase, 7 nanokatal of pyruvate kinase, 9 nanokatal of lactate dehydrogenase, and 4–1600 μM carboxylic acid substrate. For highly lipophilic substrates 0.1% Triton X-100 was added. The reaction was started by addition of 2–8 μg of purified enzyme and the oxidation of 2 mol of NADH per mol of substrate activated was followed at 340 nm (ϵ_{NADH} = 6.22 cm^2 μmol^{-1}). K_m and V_{max} values were obtained by linear regression of *V*/s against s (Hanes plots) from at least three independent experiments.

Transient Expression and Subcellular Localization of At4g05160 and At5g63380 in Planta—At4g05160 and At5g63380 cDNAs were PCR-amplified using the primer pair attB1-05160 and attB2-05160 (attB1-TCATGGAGAAATCCGGCTACGG and attB2-CTCACATCTTGGATC-TTAGTTGC) and the primer pair attB1-63380 and attB2-63380 (attB1-TCATGCTGACGAAAACCAACG and attB2-CTCAAAGTTTTGATGCA-TTGCC), respectively, thereby making the PCR products compatible with the Gateway® cloning system (Invitrogen). Both modified cDNAs were inserted into the Gateway donor vector pDONR201 by homologous recombination according to the manufacturer's instructions. The resulting plasmids were used to transfer both coding sequences into the expression vector pENSGYFP, which is based on pXCS (GenBank™ accession number AY457636) and was kindly provided by Dr. N. Medina-Escobar (Max Planck Institute for Plant Breeding Research, Köln, Germany), leading to N-terminal fusions of YFP to At4g05160 and At5g63380. To serve as peroxisomal marker, the red fluorescent protein, dsRED (FP583 from *Discosoma* sp.), with the peroxisomal import sequence -SRL fused to its C terminus (kindly provided by M. Miklis, Max Planck Institute for Plant Breeding Research, Köln, Germany) was cloned via HindIII and EcoRI restriction sites into the plant binary expression vector pAMPAT-MCS (GenBank™ accession number AY436765). All newly designed vectors allowed the *in planta* expression of proteins under the control of the constitutive cauliflower mosaic virus double 35S promoter. For transient *in planta* expression, detached leaves of 4-week-old *A. thaliana* (Col-0) plants were placed on 1% agar plates containing 85 μM benzimidazole and bombarded with 1 μm gold particles coated with vector DNA using the Biolistic® PDS-1000/He Particle Delivery System (Bio-Rad). Preparation of the DNA-coated gold beads was performed as suggested by the manufacturer. Each macrocarrier was loaded with 6 μl of the gold particle suspension, and the transformation was carried out as described previously (43). Bombarded leaves were placed in a growth chamber for 36 h, and subsequent fluorescence microscopy was carried out by using an LSM 510 Meta confocal laser microscope (Carl Zeiss, Jena, Germany). An argon laser was used as excitation source (514 nm), and light emission was detected in the range of 570–634 nm for RFP constructs and 535–545 nm for YFP constructs. Images were recorded and processed by using LSM 510 3.2 software (Carl Zeiss, Jena, Germany).

Mass Spectrometric Analysis—For the identification of the CoA ester products formed from various substrates, the reaction mixture contained 2 μg of purified enzyme, 1 mM carboxylic acid substrate, 1 mM ATP, 1 mM CoA, 30 mM NH_4HCO_3, and 0.1% Triton X-100. After an incubation period of 60 min, the samples were diluted with equal volumes of acetonitrile, and 2-μl aliquots were applied to Au/Pd-coated borosilicate glass capillary type medium (Proxeon Biosystems, Odense, Denmark). Mass spectra were recorded with a Micromass Q-TOF 2™ spectrometer (Waters) equipped with a nanoelectrospray ionization source and operating in negative ion mode. Capillary voltage was set at 800 V and cone voltage at 40 V. Full-scan mass spectra were obtained by scanning from *m/z* 0 to 1500. Putative product peaks were further characterized by MS/MS analysis using argon as collision gas and a collision voltage of 30 V. Data processing was carried out using the MassLynx software (version 3.5) from Micromass (Waters).

RNA Preparation and Collection of Gene Expression Data—*A. thaliana* plants were grown in soil in a growth chamber under controlled conditions with the photoperiod set to 10 h of light (180 $\mu E\ m^{-2}\ s^{-1}$) and 14 h of dark, a temperature of 22–23 °C, and a relative humidity of 65%. Total RNA was extracted from fully developed leaves of 4-week-old plants using RNAwiz (Ambion, Austin, Texas) according to the manufacturer's instructions. cRNA labeling, hybridization to the GeneChip ATH-1 (Affymetrix, Santa Clara, CA), and collection of fluorescence data were performed as recommended by the manufacturer. The expression value of the gene chip was scaled globally to the value of 500 arbitrary florescence units and the background set to 46.65 arbitrary florescence units.

The *Arabidopsis* cell culture At7 (derived from ecotype Columbia) was grown as described previously (44). Five days after sub-culturing, 4 mg of methyl jasmonate (MeJA; Sigma) dissolved in 0.1 ml of ethanol was added to 40 ml of cell culture. After the indicated times of incubation, cells were harvested by filtration and frozen in liquid nitrogen. Total RNA was isolated from 300 mg of cells using the RNeasy plant mini kit (Qiagen, Hilden, Germany), denatured, separated on 1.2% agarose-formaldehyde gels, transferred to nylon membranes (Biodyne B; Pall Life Sciences, New York), and hybridized with radiolabeled DNA probes as described previously (43). Equal loading was monitored by ethidium bromide staining of the gel. For semi-quantitative RT-PCR analysis, cDNA was prepared using the SuperScript cDNA synthesis kit (Invitrogen) and amplified with gene-specific primer pairs for At4g05160 (TGGAGAAATCCGGCTACGG and ATTCCATATCCCTGCATAAGC) and At5g63380 (TGACGAAAACCAACGACAGC and CGGTGGAACCT-GATAAGCC) both spanning exon-intron junctions, thereby excluding amplification of contaminating genomic DNA. Product formation was monitored after 20, 25, 30, and 35 PCR cycles by agarose gel electrophoresis. The *Arabidopsis* actin 2 gene (At3g18780) served as internal control.

Synthesis of Jasmonic Acid Precursors—OPCs were obtained as described previously (34). OPDA and dinor-OPDA were prepared from α-linolenic acid and (7*Z*,10*Z*,13*Z*)-hexadeca-7,10,13-trienoic acid, respectively, by a flaxseed extract according to Ref. 45, purified by reversed phase-high pressure liquid chromatography, and checked for purity by gas chromatography-MS. (7*Z*,10*Z*,13*Z*)-Hexadeca-7,10,13-trienoic acid could be obtained by alkaline saponification of a lipid extract from tomato leaves and separation of the 16:3 fatty acids reversed phase-high pressure liquid chromatography. All compounds represent mixtures of stereoisomers, which were used without further separation.

RESULTS

Large Scale in Vitro Substrate Analysis of Adenylate-forming Enzymes—In order to identify *in vitro* substrates of 4CL-like proteins and other carboxylic acid-activating enzymes operating via an adenylate intermediate, we established a sensitive enzyme assay, which allows the analysis of a large number of different compounds in parallel. The common feature of all adenylate-forming enzymes is the activation of their respective substrates at the expense of ATP. Correspondingly, we determined ATP consumption in a semi-quantitative assay based on luciferase-catalyzed light emission in microtiter plate format (Fig. 1*A*). To establish and optimize the assay conditions, we utilized At4CL2 (wild-type) and the At4CL2 double mutant M293P/K320L, designated PL (37, 46). At4CL2 WT efficiently activates 4-coumaric and caffeic acid to the corresponding CoA esters but exhibits strongly reduced activity toward ferulic and cinnamic acid, whereas the PL mutant readily activates all above-mentioned cinnamic acid derivatives, because of its

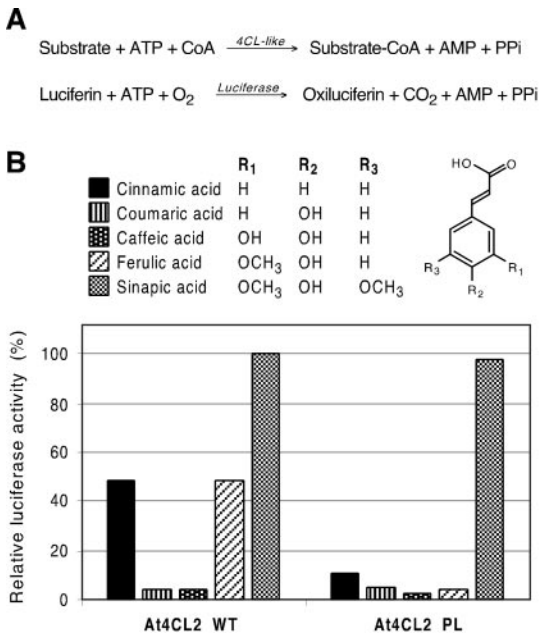

FIG. 1. **Luciferase-based activity assay of adenylate-forming enzymes.** Reaction sequence carried out for activity determination is shown. The ATP not consumed by 4CL-like proteins for CoA ester formation is used for luciferase-catalyzed bioluminescence (*A*). Affinity-purified At4CL2 wild-type (*WT*) and mutant (*PL*) enzymes were incubated for 2 h with different cinnamic acid derivatives (200 μM) in the presence of MgATP (50 μM) and CoA (100 μM), and residual ATP was determined by luciferase-dependent bioluminescence (*B*). Light emission of all assays was normalized to a reference reaction containing sinapic acid and At4CL2 WT, in which no substrate conversion and therefore no ATP depletion had occurred (100%).

larger and more hydrophobic SBP. In contrast, both At4CL2 WT and PL are completely inactive toward sinapic acid (37). The results of the optimized luciferase-based assay, as described under "Experimental Procedures," indeed reflect the known activity profiles of the At4CL2 WT and PL mutant enzymes (Fig. 1*B*). Essentially, the At4CL2 WT enzyme converted more than 95% of the ATP in mixtures containing 4-coumaric and caffeic acid during a reaction period of 2 h, whereas the PL mutant depleted ATP in mixtures containing all cinnamic acid derivatives except sinapic acid (Fig. 1*B*). Based on these results, we considered that efficient substrate conversion is indicated by a decrease in ATP concentration by more than 90% within a 2-h incubation period. Among the more than 80 additional potential substrates tested with At4CL2 WT, only 3-(4-hydroxy-phenyl)-propanoic and heptanoic acid were converted with very low efficiency, comparable with the poor substrates cinnamic and ferulic acid, characterizing At4CL2 as a highly selective enzyme (Table I).

When applied to commercially available acetyl-CoA synthetase from yeast (Roche Diagnostics), the luciferase-based assay yielded relative conversion rates of acetic, propionic, and butyric acids, which are consistent with the known properties of the enzyme (not shown). Collectively, these results demonstrate that our assay reliably reflects the properties and activities of different adenylate-forming enzymes. It is noteworthy that only a small aliquot of the reaction mixture (2 μl) was transferred to the luciferase and luciferin-containing buffer (200 μl) and that the determination of light emission was limited to the short period of 10 s. This experimental setup allowed the free variation of assay conditions for the adenylate-forming enzyme to be analyzed, while largely eliminating any interference of assay components on the luciferase-catalyzed reaction. This was an important consideration because firefly luciferase has been demonstrated recently (47) to have the

TABLE I
Substrate utilization spectrum of Arabidopsis 4CL and 4CL-like proteins

Purified recombinant proteins were incubated with more than 80 carboxylic acid substrates of which selected representatives are listed. After 2 h, the residual ATP was determined by the luciferase-based assay. Values represent relative luciferase activity, normalized to the reaction containing At4CL2 and sinapic acid in which no ATP depletion occurs (100%). Bold numbers indicate activities <10%.

Substrate	At4CL2 WT	At4g05160	At5g63380
	%	%	%
Cinnamic acid	50	118	66
4-Coumaric acid	**4**	106	50
Caffeic acid	**4**	96	69
Ferulic acid	50	128	94
Sinapic acid	100	104	120
Benzoic acid	105	129	95
2-Hydroxybenzoic acid (salicylic acid)	101	124	83
4-Hydroxybenzoic acid	115	87	120
4-Hydroxy-3,5-dimethoxybenzoic acid	96	99	69
4-Hydroxy-3-methoxybenzoic acid (vanillic acid)	101	106	94
Phenylacetic acid	97	90	81
4-Hydroxyphenylacetic acid	77	86	84
3-Phenylpropanoic acid	92	92	66
3-(4-Hydroxyphenyl)propanoic acid	34	82	66
3-(4-Hydroxy-3-methoxyphenyl)propanoic acid	120	73	78
4-Phenylbutanoic acid	127	**9**	86
4-(2-Hydroxy-4-methoxyphenyl)butanoic acid	89	93	76
5-Phenylpentanoic acid	117	**3**	59
4-Methylpentanoic acid	99	27	50
2-Hydroxy-3-phenylpropanoic acid (3-phenyllactic acid)	93	98	72
2-Hydroxyphenylacetic acid (mandelic acid)	101	77	81
Phenylalanine	98	80	92
Isoleucine	80	97	119
Succinic acid	108	87	113
Malonic acid	83	107	92
Acetic acid	87	91	85
Propanoic acid	91	103	98
Butanoic acid	97	78	86
Pentanoic acid	110	13	67
Hexanoic acid	46	**0.7**	29
Heptanoic acid	26	**3**	**8**
Octanoic acid	70	11	**7**
Nonanoic acid	54	30	**0.5**
Decanoic acid	93	13	**1**
Dodecanoic acid	109	25	**3**
Tetradecanoic acid	85	**0.6**	**0.8**
Hexadecanoic acid	94	**0.1**	**2**
Octadecanoic acid	98	**0.2**	**0.4**

intrinsic capacity to activate long-chain fatty acids. However, conversion of long-chain fatty acids was not observed in control reactions, *e.g.* with test enzymes omitted from the assays (not shown).

Structural Features of 4CL-like Genes and Proteins from A. thaliana—Phylogenetic analyses revealed that the superfamily of adenylate-forming enzymes present in *Arabidopsis* segregates into distinct clades, clearly separating the functionally identified 4CL and LACS enzymes (4, 37). Nevertheless, striking similarities were apparent between neighboring clades, for example, when comparing the structures of the *Arabidopsis* 4CL genes with their closest homologs, genes encoding 4CL-like proteins, which were previously designated as group B enzymes (37). Although the number and size of introns found in At4CL genes vary, their relative positions are conserved, *i.e.* three introns are found at identical positions in all four genes, whereas At4CL4 and At4CL3 contain one and three additional introns, respectively (Fig. 2*A*). Genes encoding 4CL-like proteins (group B) contain a similar number of introns (ranging

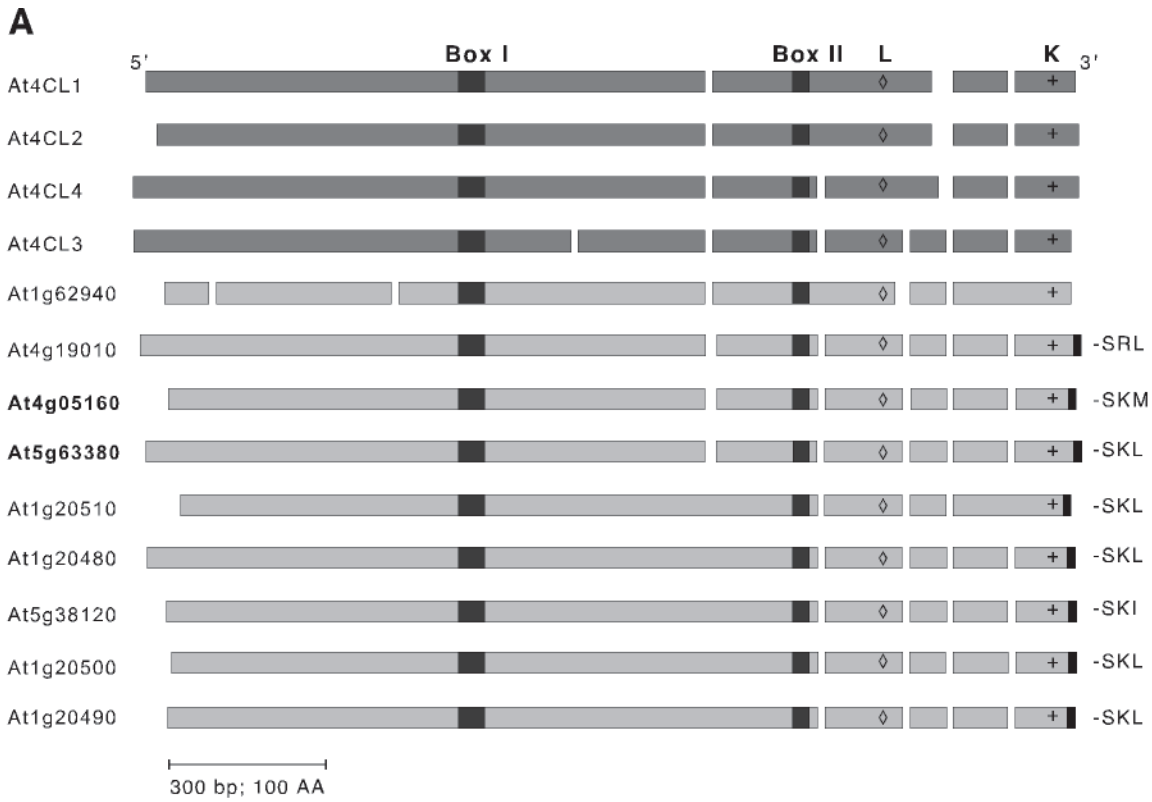

B

Cladogram	Enzyme	Amino acid position (At4CL2 numbering)												
		252	253	256	293	320	322	323	346	348	354	355	356	540
Group A	At1g51680-4CL1	Ile	Tyr	Asn	Pro	Lys	Gly	Ala	Gly	Gly	Pro	Val	Leu	Lys
	At3g21240-4CL2	Ile	Tyr	Asn	Met	Lys	Gly	Ala	Gly	Gly	Pro	Val	Leu	Lys
	At3g21230-4CL4	Ile	Tyr	Asp	Pro	Leu	Gly	Ala	Gly	Gly	Thr	Val	.	Lys
	At1g65060-4CL3	Ile	Tyr	Asn	Ala	Leu	Gly	Ala	Gly	Gly	Pro	Val	Leu	Lys
Group B	At1g62940	Ile	Tyr	Val	Pro	Met	Ala	Ala	Ala	Gly	Cys	Ile	Thr	Lys
	At4g19010	Ile	Tyr	Ser	Pro	Ser	Gly	Ala	Gly	Gly	Ala	Val	Gly	Lys
	At4g05160	Val	Phe	Ala	Trp	Gly	Gly	Ala	Gly	Gly	Gly	Ile	Val	Lys
	At5g63380	Val	Phe	Met	Pro	Gly	Gly	Gly	Gly	Gly	Gly	Pro	Ala	Lys
	At1g20510	Ile	Tyr	Ala	Pro	Leu	Gly	Gly	Gly	Gly	Gly	Ile	Gly	Lys
	At1g20480	Ile	Phe	Gly	Ser	Val	Gly	Gly	Gly	Gly	Ala	Ile	Ala	Lys
	At5g38120	Thr	Phe	Leu	Ile	Arg	Gly	Gly	Gly	Ala	Gly	Ala	Gly	Lys
	At1g20500	Thr	Tyr	Leu	Ala	Arg	Gly	Gly	Gly	Ala	Gly	Gly	Gly	Lys
	At1g20490	Ser	Phe	Leu	Ser	Arg	Gly	Gly	Gly	Ala	Gly	Ser	Gly	Lys

FIG. 2. **Structural features of genes encoding 4CLs and 4CL-like proteins from *A. thaliana* (*A*) and the substrate specificity code of the proteins (*B*).** *A*, exons are represented by *dark* (4CL, group A) and *light gray boxes* (4CL-like, group B), which are drawn to scale, whereas introns, which differ in length, are only represented by *gaps*. Conserved structural and functional domains of the encoded At4CLs and 4CL-like proteins are also shown. *Box I*, the consensus AMP-binding motif, (LIVMFY)*XX*(STG)(STAG)G(ST)(STEI)(SG)*X*(PASLIVM)(KR), and *Box II* (GEICIRG) are represented by *black boxes* (■), the L motif (DRLK(DE)L) acting as a linker between the large N- and small C-terminal domains (◊), and K, the catalytic Lys residue (+). A putative peroxisomal targeting signal of type 1 (PTS1) is present at the C terminus of most of the 4CL-like proteins and the sequence of the tripeptide is given at the right of the structure. *B*, the phylogenetic relationship of At4CLs (group A) and At4CL-like proteins (group B) is based on the amino acid sequence alignment that was generated with the PILEUP program, and the most parsimonious tree was found by using the heuristic search algorithm with the program PAUP as described previously (37). The same sequence alignment was used to extract the amino acids corresponding in position to the 12 amino acid residues that were identified previously to form the substrate-binding pocket of At4CL2 and the catalytic residue lysine 540 (37). Amino acid color code is as follows: *gray*, nonpolar side chain; *blue*, basic side chain; *red*, acidic side chain; *yellow*, polar side chain.

from 3 to 5), and most importantly, these are exclusively located at the same relative positions as in At4CL genes, with the exception of At1g62940, which carries two introns at unique sites near its 5′ end (Fig. 2*A*). The genes encoding At4g19010, At4g05160, and At5g63380 show the greatest structural similarity with the four At4CL genes. By contrast, no obvious correlation of number and position of introns could be observed between the *Arabidopsis* 4CL and LACS genes (not shown).

Based on the high sequence identity between *Arabidopsis* 4CLs and 4CL-like proteins (group B), which ranges from 37 to 44%, and based on the strictly co-linear order of highly conserved domains in both groups of enzymes (Fig. 2*A*), we considered it reasonable to apply the previously identified 12 amino acid residues comprising the 4CL substrate specificity

code to the group B proteins. We identified corresponding amino acids from multiple sequence alignments, and although it was not experimentally established that these residues indeed form the SBPs of 4CL-like proteins, we nonetheless expected to obtain hints for possible substrate preferences by this approach. In Fig. 2*B,* the phylogenetic relationship between *Arabidopsis* 4CLs (group A) and 4CL-like proteins (group B) is correlated with the properties of the putative SBP-lining amino acid residues. Two apparent and verifiable predictions arise from this analysis. First, none of the 4CL-like proteins carries a charged residue at position 256, which in At4CL2 (Asn-256) forms a hydrogen bond with the 4-hydroxy group of 4-coumaric acid (37), and correspondingly, none of the 4CL-like proteins is expected to activate 4-hydroxycinnamic acid derivatives. Second, the putative SBPs of two closely related proteins, At4g05160 and At5g63380, are exclusively made up of hydrophobic amino acids (Fig. 2*B*) and are therefore expected to preferentially bind hydrophobic substrates. We have demonstrated previously that by increasing the hydrophobicity of its SBP, At4CL2 can be converted to a cinnamic acid-activating enzyme (37), and therefore, we hypothesized that a 4CL-like protein with a hydrophobic SBP may represent a cinnamate:CoA ligase.

Two 4CL-like Proteins Function as Fatty Acyl-CoA Synthetases—To verify the hypothesis, cDNAs of both At4g05160 and At5g63380 were cloned from *Arabidopsis* (Col-0) total leaf mRNA, the encoded proteins were expressed as hexahistidine-tagged fusions in *E. coli*, and the soluble proteins were purified to apparent homogeneity by affinity chromatography under native conditions (not shown). When tested in the standard photometric 4CL assay, which records the specific absorption of the formed CoA esters, no conversion of cinnamic acid or any of its derivatives was detectable with either protein, suggesting that SBP hydrophobicity and high sequence similarity with At4CLs are insufficient criteria for cinnamic acid binding and activation. To identify true *in vitro* substrates of At4g05160 and At5g63380, we applied the luciferase-based screening assay with more than 80 candidate substrates comprising cinnamic, benzoic, amino, and fatty acid derivatives. From the results presented in Table I, it is obvious that both proteins have the capacity to activate hydrophobic substrates. Specifically, At4g05160 was active with 4-phenyl-butanoic and 5-phenyl-pentanoic acid, but derivatives having either shorter side chains, *e.g.* 3-phenyl-propanoic, phenyl-acetic, and benzoic acid, or containing additional polar groups, *e.g.* 4-(2-hydroxy-4-methoxy-phenyl)-butanoic acid, were not converted. The most efficiently activated substrates, however, were the medium-chain fatty acids, hexanoic and heptanoic acid, as well as the long-chain fatty acids, tetradecanoic (C14:0), hexadecanoic (C16:0), and octadecanoic (C18:0) acid, whereas fatty acids of intermediate chain length (octanoic, nonanoic, decanoic, and dodecanoic acid) were activated only with markedly reduced efficiency (Table I). Subsequent, detailed kinetic analyses revealed that this unusual discontinuous chain length specificity with two apparent activity maxima is because of substrate inhibition by the corresponding C8:0 to C12:0 fatty acids at the concentration applied in the luciferase-based activity assay (results not shown). At5g63380, in comparison to At4g05160, preferentially activated fatty acids with increased chain length (C9:0 to C18:0) and thus shares characteristics with long-chain fatty acyl-CoA synthetases, whereas short-chain fatty acids up to a chain length of C6, as well as phenyl-substituted fatty acids, were converted either poorly or not at all (Table I).

At4g05160 and At5g63380 Have the Capacity to Contribute to JA Biosynthesis—Although At4g05160 and At5g63380 can convert medium- and long-chain fatty acids, we were intrigued by the capacity of at least At4g05160 to also activate fatty acids carrying a bulky phenyl substitution and the fact that both proteins carry putative peroxisomal targeting signals of type 1 (PTS1) at their C termini (Fig. 2*A*). It is assumed that peroxisomal enzymes are responsible for the conversion of IBA to IAA, as well as OPDA to JA, and that both pathways include β-oxidation steps, which in analogy to fatty acid oxidation should include an activation step of the precursor to the corresponding CoA ester (21, 23, 26, 38). Based on these considerations, we extend our substrate screen. Neither At4g05160 nor At5g63380 catalyzed an appreciable conversion of indole-butyric acid (IBA), indole-propanoic acid, or IAA, indicating that both enzymes do not participate in auxin biosynthesis or metabolism (Table II). In contrast, JA precursors were activated by both enzymes, albeit with different efficiencies. The preferred substrate of At4g05160 was OPC-6:0, whereas At5g63380 converted OPDA most efficiently, which in turn was only a poor substrate for At4g05160 (Table II). Thus, the apparent preference of At4g05160 for substrates with shorter chain length, as observed with fatty acids, obviously extends to JA precursors.

TABLE II
Relative conversion rates of plant hormone precursors by Arabidopsis 4CL and 4CL-like proteins

Purified recombinant proteins were incubated for 2 h with the substrates listed, and residual ATP was determined by the luciferase-based assay. Values represent relative luciferase activity, normalized to the reaction containing At4CL2 and sinapic acid in which no ATP depletion occurs (100%). Bold numbers indicate activities <10%.

Substrate	At4CL2 WT	At4g05160	At5g63380
	%	%	%
OPDA	102	21	**0.2**
DnOPDA	93	34	104
OPC-8:0	111	41	22
OPC-6:0	96	**5**	82
OPC-4:0	95	47	90
JA	96	109	113
Indole-butyric acid	110	59	89
Indole-propionic acid	80	92	120
Indole-acetic acid	105	99	114

In view of the fact that OPDA and OPC-6:0 represent rather unusual substrates for acyl-CoA synthetases and enzymes catalyzing their activation have not previously been described, we wanted to demonstrate unequivocally that the ultimate reaction products are indeed CoA esters and exclude the possibility that the reaction stops at the level of adenylate formation. Enzymes that function solely as long-chain fatty acyl-AMP ligases and have no intrinsic capacity to form a CoA ester end product have recently been identified in *Mycobacterium tuberculosis* (48). Therefore, we determined the chemical nature of the reaction products formed from OPDA by At5g63380 by using mass spectrometry operating in negative ion mode (Fig. 3). The molecular masses of the product ions *m/z* 1040.48 and 519.63 were identical, within the experimental error, to the calculated masses of singly and doubly deprotonated OPDA-CoA (Fig. 3*B*). Both product ions were selected for fragmentation, and in the corresponding MS/MS spectra the majority of ions could be assigned to typical fragments of phosphoadenosine containing compounds (49) and fragments containing OPDA (Fig. 3*C*). Corresponding results were obtained with OPC-6:0, hexanoic, and nonanoic acid upon incubation with At4g05160 (not shown). In conclusion, compelling evidence was provided that both enzymes, At4g05160 and At5g63380, catalyze the conversion of their substrates to the CoA esters.

Catalytic Efficiency of At4g05160 and At5g63380—For enzymes accepting multiple substrates, critical assessment of substrate specificity and utilization required detailed kinetic

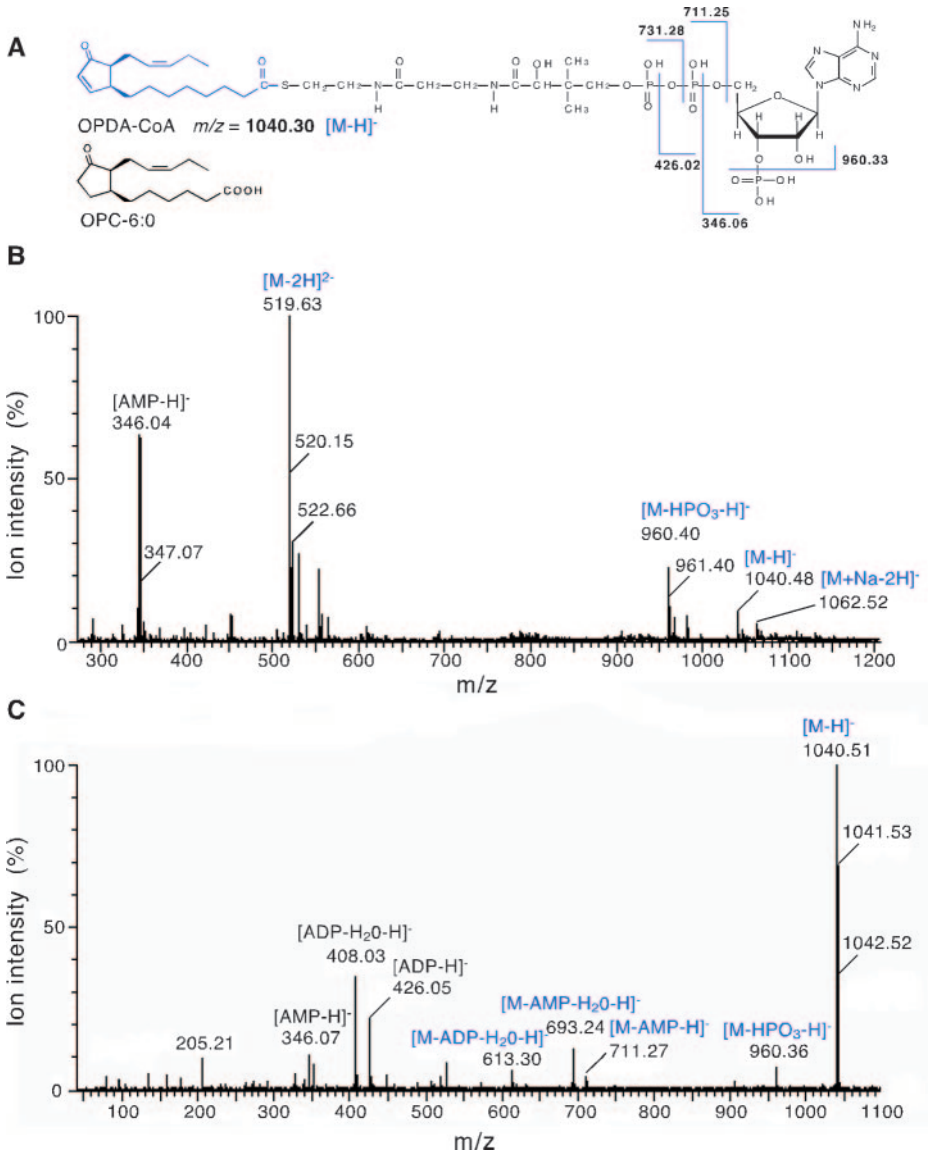

FIG. 3. **Electrospray ionization-mass spectrometric analysis of OPDA-CoA.** Structure of OPDA-CoA (M_r 1041.31), and OPC-6:0 for comparison, with the cleavage sites and *m/z* values of the major negative fragmentation ions (*A*). Full scan mass spectra of a reaction mixture containing OPDA (1 mM), MgATP (1 mM), and CoA (1 mM) were recorded in negative ion mode before and 60 min after addition of affinity-purified At5g63380 protein. The reaction product OPDA-CoA is represented in the difference spectrum by the molecular ions $[M-H]^{-1}$ (*m/z* 1040.48) and $[M-2H]^{-2}$ (*m/z* 519.63) and the fragments $[M-H_2PO_3]^{-1}$ (*m/z* 960.36) and $[AMP\text{-}H]^{-1}$ (*m/z* 346.04) derived thereof (*B*). The singly charged OPDA-CoA ion (*m/z* 1040.48) was selected for fragmentation, and the product ions were recorded in negative ion mode (*C*). This MS/MS analysis resulted in fragments characteristic of CoA or phosphoadenosine-containing compounds, such as $[AMP\text{-}H]^{-1}$ (*m/z* 346.07), $[ADP\text{-}H]^{-1}$ (*m/z* 426.05), and $[ADP\text{-}H_2O\text{-}H]^{-1}$ (*m/z* 408.03), in addition to fragments containing OPDA, such as $[M-H_2PO_3]^{-1}$ (*m/z* 960.36), $[M-AMP\text{-}H]^{-1}$ (*m/z* 711.27), $[M-AMP\text{-}H_20\text{-}H]^{-1}$ (*m/z* 693.24), and $[M-ADP\text{-}H_2O\text{-}H]^{-1}$ (*m/z* 613.30), thereby confirming the structure of the product OPDA-CoA.

parameters. To establish such data, we applied a quantitative photometric assay, which couples the rate of AMP formation by adenylate-forming enzymes to NADH oxidation via the auxiliary enzymes myokinase, pyruvate kinase, and lactate dehydrogenase (42). For both 4CL-like proteins the kinetic parameters (K_m and k_{cat}) were determined for two medium-chain (C6:0, C9:0) and one long-chain fatty acid (C14:0), as well as for the JA precursors OPDA and OPC-6:0 (Table III). From the data in Table III, it is evident that At4g05160 functions as fatty acyl-CoA synthetase with a preference for substrates of medium-chain length. With a k_{cat}/K_m value of 230.6, nonanoic acid represents the most efficiently converted substrate, but hexanoic (k_{cat}/K_m = 16.74) and tetradecanoic acid (k_{cat}/K_m = 42.76) were also converted with appreciable efficiency. Both OPDA and OPC-6:0 have comparable but significantly lower k_{cat}/K_m values than the fatty acids used in this analysis (Table III).

In the case of At5g63380, the efficiency of fatty acid activation increases continuously with their chain length, with k_{cat}/K_m values of 0.44, 9.35, and 57.19 for hexanoic, nonanoic, and tetradecanoic acid, respectively, resulting in a preliminary classification of this enzyme as LACS. In fact, the activity of both At5g63380 as well as At4g05160 with long-chain fatty acids compares favorably with those of other LACS enzymes of plant origin (4, 10, 12, 50). However, the low K_m of 11 μM and the high k_{cat}/K_m value of 237.9 determined for OPDA (Table II) justify the classification of At5g63380 as a *bona fide* OPDA:CoA ligase. In contrast to At4g05160, the activity of At5g63380 with OPC-6:0 was too low to allow a reliable determination of kinetic parameters. In agreement with the data presented in Table I, activation of fatty acids by At4CL2 was not detectable.

Expression Level and Subcellular Localization of At4g05160 and At5g63380—Because JA is synthesized from OPDA or dinor-OPDA in peroxisomes, enzymes contributing to this conversion must be expressed at reasonable levels and targeted to this organelle. To verify whether or not At4g05160 and At5g63380 fulfil both of these criteria, we analyzed their expression and subcellular localization. Steady state mRNA levels of At4g05160 and At5g63380 in *Arabidopsis* leaves were considerably higher than those of all other members of group B proteins, except At1g20510 and At1g20490, reaching 20–60% of the expression level exhibited by At4CL1 (Fig. 4). At4CL1 has been shown previously (6) to represent the most abundant 4CL isoform in leaves. Although mRNA levels need not necessarily correlate with protein abundance, we conclude that At4g05160 and At5g63380 are presumably of functional importance. The expression of At4g05160 and At5g63380 in other plant organs was determined by semi-quantitative RT-PCR. The results revealed that both genes are co-expressed and that

TABLE III

Kinetic properties of the A. thaliana proteins At4g05160 and At5g63380

Enzyme activity was determined by the lactate dehydrogenase-coupled assay with affinity-purified proteins and varied concentrations of the substrates listed. All values are the mean ± S.D. of at least three independent determinations.

Substrate	At4g05160			At5g63380		
	K_m	k_{cat}	k_{cat}/K_m	K_m	k_{cat}	k_{cat}/K_m
	μM	s^{-1}	$s^{-1}\ mM^{-1}$	μM	s^{-1}	$sec^{-1}\ mM^{-1}$
Hexanoic acid	75 ± 18	1.26 ± 0.09	16.74	6302 ± 1548	2.79 ± 0.25	0.44
Nonanoic acid	6 ± 1	1.38 ± 0.12	230.65	2125 ± 1700	19.87 ± 9.68	9.35
Tetradecanoic acid	54 ± 7	2.31 ± 0.47	42.76	35 ± 10	2.00 ± 0.16	57.19
OPDA	93 ± 36	0.30 ± 0.08	3.19	11 ± 5	2.62 ± 0.93	237.86
OPC-6:0	187 ± 33	0.41 ± 0.06	2.19	ND[a]	ND	ND

[a] ND, not determined, activity too low.

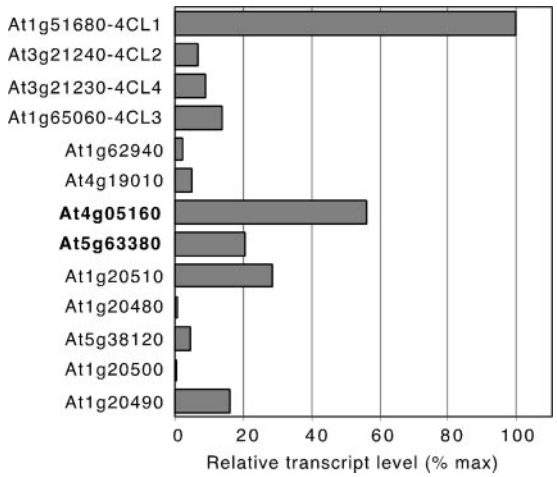

FIG. 4. **Expression levels of At4CLs and At4CL-like genes in *Arabidopsis* leaves.** Total RNA was extracted from fully developed leaves of 4-week-old *Arabidopsis* plants, and relative transcript levels were determined as described under "Experimental Procedures."

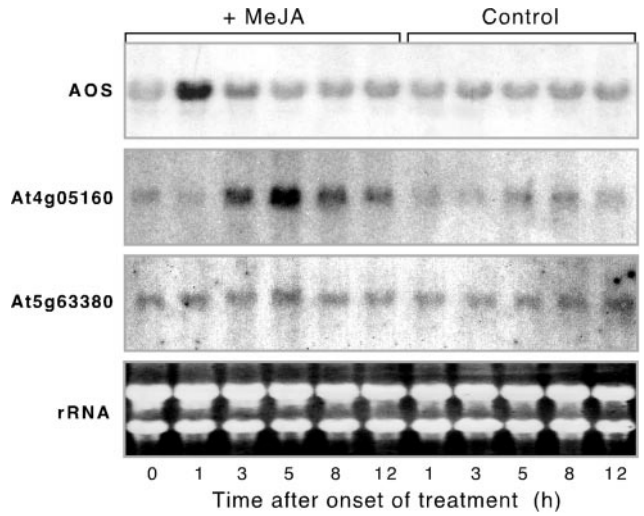

FIG. 5. **Influence of methyl jasmonate on gene expression in cultured *Arabidopsis* cells.** Cultured *Arabidopsis* cells were treated with MeJA (final concentration 100 μg/ml) and incubated for the times indicated. Control cultures were mock-treated and kept in parallel under otherwise identical conditions. Total extractable RNA was separated on agarose gels (30 μg/lane), blotted onto nylon membranes, and hybridized with radiolabeled probes. Equal RNA loading was monitored by ethidium bromide staining.

leaves, stems, and flowers contained comparable mRNA amounts, whereas those in roots and siliques were significantly lower (results not shown).

It its known that jasmonates induce the expression of genes encoding enzymes of JA biosynthesis such as lipoxygenase, allene oxide synthase, allene-oxide cyclase-2, and OPR-3 (28). To explore whether At4g05160 and At5g63380 are also part of this proposed positive feedback regulatory system, we analyzed their expression in cultured *Arabidopsis* cells in response to MeJA treatment. As is obvious from Fig. 5, the amount of At4g05160 mRNA increased strongly and transiently under these conditions, although with a delay in comparison to allene oxide synthase mRNA accumulation, whereas the expression At5g63380 was not affected by MeJA treatment.

When inspecting the N-terminal regions of At4g05160 and At5g63380 for subcellular targeting signal sequences, no such peptide motifs were identified. However, both proteins possess major peroxisomal targeting signals of type 1 (PTS1) at their C termini (Fig. 2*A*). To demonstrate that the C-terminal tripeptides present in At4g05160 (−SKM) and At5g63380 (−SKL) in fact target their enzymes to peroxisomes, we constructed fusion proteins containing spectral variants of the green fluorescent protein and used these for transient expression and double labeling experiments. RFP extended by the canonical major PTS1 tripeptide -SRL (RFP-SRL) was used as peroxisomal marker protein, because a corresponding green fluorescent protein variant has been shown previously (51–54) to be successfully targeted to the organelle in yeast, mammalian, and plant cells. The complete coding sequences of At4g05160 or At5g63380 were fused to the C terminus of YFP, and all constructs placed under the control of the cauliflower mosaic virus 35S promoter (Fig. 6*A*). For co-localization studies, *Arabidopsis* leaves were biolistically transformed with RFP-SRL and YFP-At4g05160 or YFP-At5g63380, and after a 36-h post-bombardment period, single cells inspected by confocal laser-scanning microscopy. Transformed cells showed a punctate labeling pattern, which is characteristic for peroxisomes (Fig. 6). The complete three-dimensional co-localization of yellow and red fluorescence, originating from YFP-At4g05160/YFP-At5g63380 and RFP-SRL, respectively, provides compelling evidence that both At4g05160 and At5g63380 are localized in peroxisomes (Fig. 6, *C* and *F*), *i.e.* in the organelle that is responsible for fatty acid β-oxidation and the final steps of JA biosynthesis.

DISCUSSION

To decipher the function of large sets of new, uncharacterized proteins and enzymes that are amply predicted from whole genome sequences is a major challenge of the post-genomic decade that will provide the basis for our understanding of complex biological phenomena, such as regulatory networks, biosynthetic pathways, substrate channeling, and the coordination of metabolic flux within cells. We are currently investigating the biochemical properties and functions of proteins belonging to a large family of so-called adenylate-forming enzymes, which is characterized by the presence of a consensus AMP-binding motif (PROSITE PS00455). In the *Arabidopsis* genome, this group consists of at least 44 proteins, which are organized in six phylogenetic clades (4). At present, the biochemical properties of 16 of these proteins have been studied in

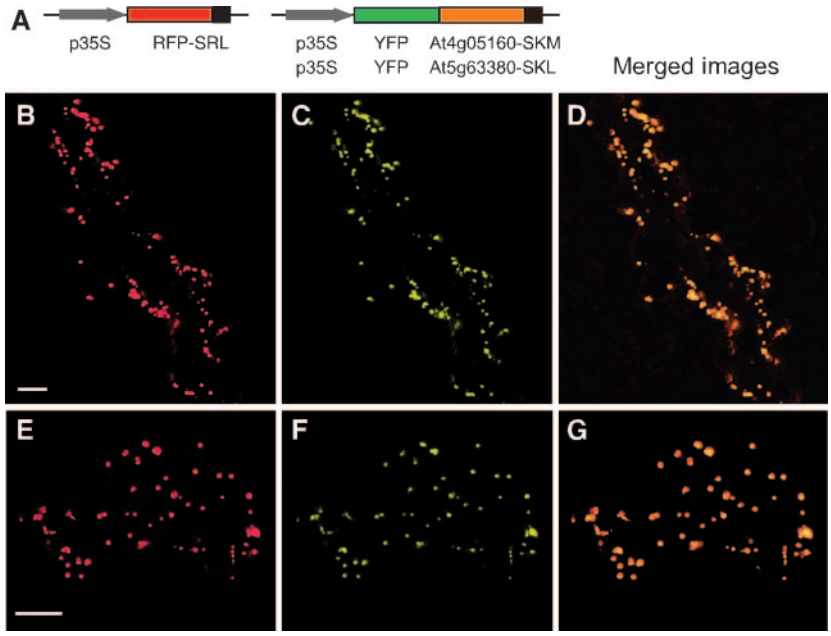

FIG. 6. **Subcellular localization of At4g05160 and At5g63380 proteins in *Arabidopsis* leaves.** Expression plasmids harboring YFP-At4g05160 or YFP-At5g63380 (*A*) under the control of the cauliflower mosaic virus 35S promoter (*p35S*) were co-transformed with p35S::RFP-SRL (*A*) into *Arabidopsis* leaves by particle bombardment. Single epidermal cells were inspected by confocal laser microscopy using appropriate filter sets for simultaneous and selective recording of RFP (*B* and *E*) and YFP (*C* and *F*) fluorescence, and 16 optical sections were used for the reconstruction of three-dimensional images of the cells. The punctate labeling patterns of RFP (peroxisomal marker) and YFP (4CL-like proteins) are virtually identical as evident from the *orange color* of the merged images (*D* and *G*), clearly demonstrating the peroxisomal localization of the 4CL-like proteins. The *scale bars* represent 20 μm.

detail. Enzymes characterized so far comprise nine long-chain and two short-chain fatty acyl-CoA synthetases, a single acetyl-CoA synthetase, and four 4CLs (4, 6–13). The function of the remaining proteins is unknown, although the presence of the conserved AMP-binding domain suggests that they also catalyze CoA ester formation via an adenylate intermediate.

In order to identify the substrates of these putative CoA ligases we established a general assay for adenylate-forming enzymes by exploiting their common feature, which is the ATP dependence of the first half-reaction (Reaction 1). Luciferase has been widely used both as reporter for gene expression studies and an auxiliary enzyme for ATP determination by bioluminescence. By using 4CL variants with specific substrate utilization patterns, we optimized the conditions in order to establish a sensitive and versatile assay that is suitable for screening different enzymes of unknown catalytic efficiency and activity optima with a large number of potential substrates. Assay sensitivity was of particular concern during optimization in view of the fact that catalytic activities of enzymes can vary enormously, and turnover numbers are known to differ by several orders of magnitude (55). The sensitivity of the luciferase-based assay can easily be modulated by varying the incubation period of enzymes catalyzing CoA ester formation. Consequently, only a fraction of the reaction mixture was used for ATP determination, thereby allowing repetitive sampling in a temporal window ranging from a few minutes to several hours. Furthermore, under these conditions the formation of uncommon mono- and diadenosine polyphosphates, a side reaction of 4CLs and other enzymes forming acyl-adenylate intermediates, can be excluded (56).

The great versatility that is offered by the luciferase-based assay has not yet been fully exploited by our experimental approach, which aimed at identifying substrates that are converted to the CoA ester. However, a number of enzymes have recently been identified that catalyze either only the synthesis of the adenylate intermediate without subsequent transfer of the activated acid to an acceptor or utilize acceptors other than CoA. Enzymes of this kind include fatty acyl-AMP ligases from *M. tuberculosis* and jasmonate:isoleucine aminotransferase (JAR1) from *A. thaliana* (5, 48). Pilot experiments indicate that omission of CoA from the assay mixture will make it feasible to identify substrates that are only converted to the adenylate, if pyrophosphate (PP_i) is removed from the equilibrium of the first half-reaction (Reaction 1). Such a modified assay will allow us to screen first for a substrate that is converted to an adenylate and second for alternative acceptor molecules different from CoA.

By applying the substrate screening procedure to two selected 4CL-like proteins, we uncovered that At4g05160 and At5g63380 represent fatty acyl-CoA synthetases with a relatively broad specificity for medium- to long-chain fatty acids (Table I). This was an unexpected finding, because in *Arabidopsis* a family of nine *bona fide* LACS enzymes has already been characterized, and overall amino acid sequence identity of At4g05160 and At5g63380 to this group of proteins is lower than 25%. Corresponding to the disparity at the protein level, no similarity in exon/intron organization of LACS genes and the genes encoding At4g05160 and At5g63380 can be observed. In addition, several LACS proteins have been reported to contain two peptide motifs, which are responsible for substrate binding and determination of chain length specificity (57, 58). However, these motifs are not well conserved in At4g05160 and At5g63380 and therefore, based on all the above criteria, both proteins do not represent typical LACS enzymes. By contrast, At4g05160 and At5g63380 show an identical order of highly conserved peptide motifs and an overall amino acid sequence identity of about 40% when compared with *bona fide Arabidopsis* 4CLs. Furthermore, the exon/intron organization of both types of genes is almost identical (Fig. 2*A*).

Based on our recent results that At4CL2 can be converted to a cinnamic acid-activating enzyme by increasing the hydrophobicity of its substrate-binding pocket (37), and based on the observation that the putative SBPs of At4g05160 or At5g63380 are exclusively formed by hydrophobic amino acids, we hypothesized that either one or both proteins may represent a missing cinnamate:CoA ligase, a potential enzyme of salicylic acid biosynthesis via the phenylpropanoid pathway (59–62). However, our results demonstrate that neither At4g05160 nor At5g63380 converted cinnamic acid to any significant extent (Table I). Although At4g05160 and At5g63380 are structurally closely related to 4CLs, *i.e.* enzymes of secondary metabolism, their *in vitro* catalytic activities are comparable with those of fatty acyl-CoA synthetases, *i.e.* enzymes of primary metabolism. A generally accepted hypothesis postulates that enzymes of secondary metabolism have evolved from ancestors necessary for primary metabolism. Consequently, it has been suggested that

firefly luciferase evolved from an ancestral LACS and therefore has kept its principal capacity for activation of fatty acids (47, 63). However, At4CL2, which exhibits significant sequence similarity with luciferase, has apparently lost the capacity to activate fatty acids, whereas the closely related 4CL-like proteins, At4g05160 and At5g63380, have retained this capacity, indicating a high evolutionary plasticity of adenylate-forming enzymes with respect to their substrate utilization spectra.

Enzymes of general phenylpropanoid metabolism, including 4CL, are cytosolic proteins or part of protein complexes that assemble at the cytosolic side of microsomal membranes (64, 65). By contrast, all 4CL-like proteins (group B), except At1g62940, carry major C-terminal peroxisomal targeting signals (PTS1) as recently defined for *Arabidopsis* (66); for At4g05160 and At5g63380 we verified the functionality of the PTS1 (Fig. 6). The observation that At4g05160 and At5g63380 are peroxisomal fatty acyl-CoA synthetases and that At4g05160 has the catalytic capacity to activate some medium-chain fatty acids carrying a bulky substituent, such as 4-phenyl-butanoic and 5-phenyl-pentanoic acid, provided the experimental lead for extending the substrate screen to compounds such as auxin derivatives and jasmonic acid precursors. IBA is suggested to be converted to IAA by the peroxisomal β-oxidation system, and consequently, several *Arabidopsis* mutants with impaired β-oxidation exhibit an enhanced tolerance to otherwise toxic concentrations of IBA or of the proherbicide 2,4-diphenoxy-butyric acid (21, 67). However, neither At4g05160 nor At5g63380 showed activation of IBA, indolepropanoic acid, or IAA to any significant extent (Table II). By contrast, the JA precursors, OPDA and OPC-6:0, were converted to their CoA esters by At4g05160 with appreciable efficiency, albeit lower than the conversion of fatty acids, whereas At5g63380 exhibited high activity toward OPDA, whereas OPC-6:0 was not converted (Table III). Most importantly, OPDA was the most efficiently converted of all tested substrates, thereby characterizing At5g63380 as an OPDA:CoA ligase. In view of the fact that the biochemical pathway of JA biosynthesis is well established and all participating enzymes have been identified, with the exception of those initiating and catalyzing the β-oxidative chain shortening, this is an important finding. In general, fatty acids are thought to cross membranes as CoA esters, although translocation of medium-chain fatty acids to yeast peroxisomes and of at least a fraction of the long-chain fatty acids to *Arabidopsis* peroxisomes occurs at the level of free acids (12, 13, 68). Furthermore, the recent discovery of peroxisomal fatty acyl-CoA thioesterases may indicate unanticipated high levels of free fatty acids and CoA within peroxisomes (69). It is therefore conceivable that OPDA is either imported by peroxisomes prior to CoA ester formation or that it is released from its CoA ester within the organelle after translocation from the cytoplasm. Obviously, both scenarios imply the participation of peroxisomal CoA ligases in JA production. In fact, At4g05160 and At5g63380 fulfill several criteria of enzymes involved in JA biosynthesis, including their capacity to activate JA precursors to the corresponding CoA esters and their co-localization in the relevant organelle. Although only At4g05160 but not At5g63380 displays jasmonate-inducible expression typical of JA biosynthetic enzymes, the organ-specific co-expression of their genes and co-localization of the enzymes *in planta* together with their substrate specificities suggest that they have a cooperative function in providing the cell with activated JA precursors. The observation that closely related CoA ligases participating in one product-specific pathway are differentially regulated is not unusual and has been described for the acetyl:CoA synthetase isoforms ACS1 and ACS2 from yeast (70).

The current scheme of JA biosynthesis suggests that OPDA and probably dinor-OPDA are reduced to OPC-8:0 and OPC-6:0, respectively, by the enzyme OPR-3, which is localized in peroxisomes (22, 25, 33). Correspondingly, the reaction products, OPC-8:0 and OPC-6:0, would require activation to the CoA ester to initiate the β-oxidative chain shortening leading to JA (25). The capacity of At4g05160 to activate at least OPC-6:0 is in accordance with the proposed function, whereas an enzyme active toward OPC-8:0 remains to be identified. Alternatively, if At5g63380 participates in JA biosynthesis by activation of OPDA, the implication is that reduction of OPDA to OPC-8:0 occurs at the level of the CoA ester. To our knowledge it is presently unknown whether or not OPR-3 has the capacity to reduce not only the free acid but also the CoA ester.

Although our data support a participation of 4CL-like proteins in JA biosynthesis, their involvement in other functions cannot be dismissed. In contrast to At4CL2, which is a highly selective enzyme with clearly defined *in vitro* substrate specificity, both At4g05160 and At5g63380 in addition to JA precursors also activate various medium- and long-chain fatty acids (Table I). The capacity to activate different fatty acid derivatives, including fatty acids carrying a phenyl substitution, is reminiscent of so-called xenobiotic fatty acid:CoA ligases found in animals, which contribute to the detoxification of lipophilic compounds by their activation to CoA esters and subsequent conjugation with amino acids (71, 72). Therefore, At4g05160 and At5g63380 may have functions distinct from JA biosynthesis, such as activation of fatty acids for conjugation with other molecules or even activation of fatty acids released from storage lipids for production of acetyl-CoA. However, the latter reaction is apparently of no physiological relevance, because the *Arabidopsis lacs6 lacs7* double mutant, which is defective in the two peroxisomal isoforms of the LACS enzyme family, is specifically impaired in β-oxidation of fatty acids released from storage lipids despite the presence of At4g05160 and At5g63380 (13).

Both At4g05160 and At5g63380 show a similar organ-specific expression pattern and, with respect to fatty acid activation, a relatively broad and overlapping substrate utilization profile, which in combination with the other known fatty acyl-CoA synthetases in *Arabidopsis* may form a redundant enzymatic system for fatty acid activation. Such a system is probably not only required for the degradation of storage lipids but also for the generation, modification, or degradation of lipid-derived signal molecules. The latter function can be associated with At4g05160 and At5g63380. In fact, both proteins are the first for which the *in vitro* capacity for activation of JA precursors has been demonstrated. Their apparent selective activation of different JA precursors raises the intriguing question whether subsequent reactions are also catalyzed by specific enzymes or by the general β-oxidation machinery. Obviously, the biological significance of the reactions catalyzed by At4g05160 and At5g63380 still needs to be addressed. For this purpose, the isolation of knock-out mutants for both genes will be essential. Such mutants are predicted to exhibit both phenotypic and biochemical alterations related to JA function or biosynthesis, such as male sterility, modification of marker gene expression, and the oxylipin signature, provided that a nonredundant function is affected. However, a more realistic expectation is that combinations of defective genes are required to establish a phenotype, similar to the recently described *Arabidopsis lacs6 lacs7* double mutant (13). The functions of most 4CL-like proteins and many other adenylate-forming enzymes remain unknown, and the combination of genetic and biochemical approaches will be required to uncover their biological importance. The screening procedure for *in vitro* sub-

strate utilization presented in this work will be a useful tool to identify the biochemical functions of uncharacterized adenylate-forming enzymes, thereby defining groups of proteins with identical, overlapping or unique substrate preferences and utilization profiles. This information will be key for designing reverse genetic approaches involving double and multiple mutant analysis.

Acknowledgments—We thank Dr. Imre E. Somssich for critical comments on the manuscript and Brigitte Pickel and Roswitha Lentz for excellent technical assistance.

REFERENCES

1. Fulda, M., Heinz, E., and Wolter, F. P. (1994) *Mol. Gen. Genet.* **242,** 241–249
2. Stuible, H.-P., Büttner, D., Ehlting, J., Hahlbrock, K., and Kombrink, E. (2000) *FEBS Lett.* **467,** 117–122
3. Staswick, P. E., Tiryaki, I., and Rowe, M. L. (2002) *Plant Cell* **14,** 1405–1415
4. Shockey, J. M., Fulda, M. S., and Browse, J. (2003) *Plant Physiol.* **132,** 1065–1076
5. Staswick, P. E., and Tiryaki, I. (2004) *Plant Cell* **16,** 2117–2127
6. Ehlting, J., Büttner, D., Wang, Q., Douglas, C. J., Somssich, I. E., and Kombrink, E. (1999) *Plant J.* **19,** 9–20
7. Shockey, J. M., Fulda, M. S., and Browse, J. A. (2002) *Plant Physiol.* **129,** 1710–1722
8. Ke, J., Behal, R. H., Back, S. L., Nikolau, B. J., Wurtele, E. S., and Oliver, D. J. (2000) *Plant Physiol.* **123,** 497–508
9. Hamberger, B., and Hahlbrock, K. (2004) *Proc. Natl. Acad. Sci. U. S. A.* **101,** 2209–2214
10. Schnurr, J. A., Shockey, J. M., de Boer, G.-J., and Browse, J. A. (2002) *Plant Physiol.* **129,** 1700–1709
11. Schnurr, J., Shockey, J., and Browse, J. (2004) *Plant Cell* **16,** 629–642
12. Fulda, M., Shockey, J., Werber, M., Wolter, F. P., and Heinz, E. (2002) *Plant J.* **32,** 93–103
13. Fulda, M., Schnurr, J., Abbadi, A., Heinz, E., and Browse, J. (2004) *Plant Cell* **16,** 394–405
14. Zolman, B. K., Silva, I. D., and Bartel, B. (2001) *Plant Physiol.* **127,** 1266–1278
15. Hayashi, M., Toriyama, K., Kondo, M., and Nishimura, M. (1998) *Plant Cell* **10,** 183–196
16. Germain, V. (2001) *Plant J.* **28,** 1–12
17. Graham, I. A., and Eastmond, P. J. (2002) *Prog. Lipid Res.* **41,** 156–181
18. Lange, P. R., Eastmond, P. J., Madagan, K., and Graham, I. A. (2004) *FEBS Lett.* **571,** 147–153
19. Zolman, B. K., Monroe-Augustus, M., Thompson, B., Hawes, J. W., Krukenberg, K. A., Matsuda, S. P. T., and Bartel, B. (2001) *J. Biol. Chem.* **276,** 31037–31046
20. Corpas, F. J., Barroso, J. B., and del Rio, L. A. (2001) *Trends Plant Sci.* **6,** 145–150
21. Zolman, B. K., Yoder, A., and Bartel, B. (2000) *Genetics* **156,** 1323–1337
22. Stintzi, A., and Browse, J. (2000) *Proc. Natl. Acad. Sci. U. S. A.* **97,** 10625–10630
23. Bartel, B., LeClere, S., Magidin, M., and Zolman, B. K. (2001) *J. Plant Growth Regul.* **20,** 198–216
24. Hayashi, M., and Nishimura, M. (2003) *Curr. Opin. Plant Biol.* **6,** 577–582
25. Weber, H. (2002) *Trends Plant Sci.* **7,** 217–224
26. Turner, J. G., Ellis, C., and Devoto, A. (2002) *Plant Cell* **14,** S153–S164
27. Ishiguro, S., Kawai-Oda, A., Ueda, J., Nishida, I., and Okada, K. (2001) *Plant Cell* **13,** 2191–2209
28. Stenzel, I., Hause, B., Miersch, O., Kurz, T., Maucher, H., Weichert, H., Ziegler, J., Feussner, I., and Wasternack, C. (2003) *Plant Mol. Biol.* **51,** 895–911
29. Howe, G. A., and Schilmiller, A. L. (2002) *Curr. Opin. Plant Biol.* **5,** 230–236
30. Stelmach, B. A., Müller, A., Hennig, P., Gebhardt, S., Schubert-Zsilavecz, M., and Weiler, E. W. (2001) *J. Biol. Chem.* **276,** 12832–12838
31. Stintzi, A., Weber, H., Reymond, P., Browse, J., and Farmer, E. E. (2001) *Proc. Natl. Acad. Sci. U. S. A.* **98,** 12837–12842
32. Schaller, F. (2001) *J. Exp. Bot.* **52,** 11–23
33. Sanders, P. M., Lee, P. Y., Biesgen, C., Boone, J. D., Beals, T. P., Weiler, E. W., and Goldberg, R. B. (2000) *Plant Cell* **12,** 1041–1062
34. Miersch, O., and Wasternack, C. (2000) *Biol. Chem.* **381,** 715–722
35. Douglas, C. J. (1996) *Trends Plant Sci.* **1,** 171–178
36. Weisshaar, B., and Jenkins, G. I. (1998) *Curr. Opin. Plant Biol.* **1,** 251–257
37. Schneider, K., Hövel, K., Witzel, K., Hamberger, B., Schomburg, D., Kombrink, E., and Stuible, H.-P. (2003) *Proc. Natl. Acad. Sci. U. S. A.* **100,** 8601–8606
38. Reumann, S., Ma, C., Lemke, S., and Babujee, L. (2004) *Plant Physiol.* **136,** 2587–2608
39. Bradford, M. M. (1976) *Anal. Biochem.* **72,** 248–254
40. Gross, G. G., and Zenk, M. H. (1966) *Z. Naturforsch.* **21,** 683–690
41. Stöckigt, J., and Zenk, M. H. (1975) *Z. Naturforsch.* **30,** 352–358
42. Ziegler, K., Braun, K., Böckler, A., and Fuchs, G. (1987) *Arch. Microbiol.* **149,** 62–69
43. Ancillo, G., Hoegen, E., and Kombrink, E. (2003) *Planta* **217,** 566–576
44. Hartmann, U., Valentine, W. J., Christie, J. M., Hays, J., Jenkins, G. I., and Weisshaar, B. (1998) *Plant Mol. Biol.* **36,** 741–754
45. Vick, B. A., Feng, P., and Zimmerman, D. C. (1980) *Lipids* **15,** 468–471
46. Stuible, H.-P., and Kombrink, E. (2001) *J. Biol. Chem.* **276,** 26893–26897
47. Oba, Y., Ojika, M., and Inouye, S. (2003) *FEBS Lett.* **540,** 251–254
48. Trivedi, O. A., Arora, P., Sridharan, V., Tickoo, R., Mohanty, D., and Gokhale, R. S. (2004) *Nature* **428,** 441–445
49. Mauriala, T., Herzig, K. H., Heinonen, M., Idziak, J., and Auriola, S. (2004) *J. Chromatogr. B* **808,** 263–268
50. Fulda, M., Heinz, E., and Wolter, F. P. (1997) *Plant Mol. Biol.* **33,** 911–922
51. Brocard, C., Lametschwandtner, G., Koudelka, R., and Hartig, A. (1997) *EMBO J.* **16,** 5491–5500
52. Kragler, F., Lametschwandtner, G., Christmann, J., Hartig, A., and Harada, J. J. (1998) *Proc. Natl. Acad. Sci. U. S. A.* **95,** 13336–13341
53. Mano, S., Nakamori, C., Hayashi, M., Kato, A., Kondo, M., and Nishimura, M. (2002) *Plant Cell Physiol.* **43,** 331–341
54. Mohan, K. V. K., Som, I., and Atreya, C. D. (2002) *J. Virol.* **76,** 2543–2547
55. Fersht, A. (1985) *Enzyme Structure and Mechanism*, 2nd Ed., W. H. Freeman & Co., New York
56. Pietrowska-Borek, M., Stuible, H.-P., Kombrink, E., and Guranowski, A. (2003) *Plant Physiol.* **131,** 1401–1410
57. Black, P. N., Zhang, Q., Weimar, J. D., and DiRusso, C. C. (1997) *J. Biol. Chem.* **272,** 4896–4903
58. Black, P. N., DiRusso, C. C., Sherin, D., MacColl, R., Knudsen, J., and Weimar, J. D. (2000) *J. Biol. Chem.* **275,** 38547–38553
59. León, J., Shulaev, V., Yalpani, N., Lawton, M., and Raskin, I. (1995) *Proc. Natl. Acad. Sci. U. S. A.* **92,** 10413–10417
60. Lee, H.-I., León, J., and Raskin, I. (1995) *Proc. Natl. Acad. Sci. U. S. A.* **92,** 4076–4079
61. Mauch-Mani, B., and Slusarenko, A. J. (1996) *Plant Cell* **8,** 203–212
62. Wildermuth, M. C., Dewdney, J., Wu, G., and Ausubel, F. M. (2001) *Nature* **414,** 562–565
63. Hisanaga, Y., Ago, H., Nakagawa, N., Hamada, K., Ida, K., Yamamoto, M., Hori, T., Arii, Y., Sugahara, M., Kuramitsu, S., Yokoyama, S., and Miyano, M. (2004) *J. Biol. Chem.* **279,** 31717–31726
64. Dixon, R. A., Chen, F., Guo, D., and Parvathi, K. (2001) *Phytochemistry* **57,** 1069–1084
65. Winkel, B. S. J. (2004) *Annu. Rev. Plant Biol.* **55,** 85–107
66. Reumann, S. (2004) *Plant Physiol.* **135,** 783–800
67. Zolman, B. K., and Bartel, B. (2004) *Proc. Natl. Acad. Sci. U. S. A.* **101,** 1786–1791
68. Hettema, E. H., and Tabak, H. F. (2000) *Biochim. Biophys. Acta* **1486,** 18–27
69. Tilton, G. B., Shockey, J. M., and Browse, J. (2004) *J. Biol. Chem.* **279,** 7487–7494
70. Hiesinger, M., Wagner, C., and Schüller, H.-J. (1997) *FEBS Lett.* **415,** 16–20
71. Vessey, D. A., and Kelley, M. (2001) *Biochem. J.* **357,** 283–288
72. Vessey, D. A., Lau, E., Kelley, M., and Warren, R. S. (2003) *J. Biochem. Mol. Toxicol.* **17,** 1–6